RSC Advances

ROYAL SOCIETY OF CHEMISTRY

www.rsc.org/advances

RSC Advances

RSCPublishing

ARTICLE

Cite this: DOI: 10.1039/x0xx00000x
Received ooth January 2012,
Accepted ooth January 2012
DOI: 10.1039/x0xx00000x
www.rsc.org/

Decoration of Carbon Nanotubes by Chitosan in a Nanohybrid Conductive Polymer Composite for Detection of Polar Vapours

P. Molla-Abbasi[a], S. R. Ghaffarian[a,*]

A new nanohybrid conductive composite was designed for detection of polar vapours and characterized based on thermodynamic parameters to investigate the sensor response. Poly (ethylene oxide) (PEO) and poly (vinyl alcohol) (PVA) / carbon nanotubes (CNTs) nanocomposite sensors were introduced to various organic vapours such as methanol, ethanol, isopropyl alcohol (IPA), chloroform and water. The response of these sensors was investigated based on thermodynamic parameters. Although, affinity is one of the most important parameters that can affect the response of sensors, the interaction parameter (χ) proposed by Flory and Huggins, cannot clarify the response trend for these series of nanocomposite transducers. We interpreted the response trend of transducers based on polarity contribution of Hansen solubility parameter. Thus, by designing a new nanohybrid nanocomposite, the sensor response against polar vapours was improved. New active sites in conductive polymer composites (CPCs) were designed by decoration of CNTs with chitosan (a polar biopolymer) and introducing of these new conductive particles to PVA and PEO. The wrapping of chitosan around CNTs was further investigated by molecular dynamics (MD) simulations. The polar functional groups of chitosan enhanced the driving force for diffusion of polar molecules into the nanohybrid composite and adsorption on the surface of CNTs and subsequently improved the sensor response.
.

1 Introduction

Over the past years, there has been an increasing demand for vapour sensor applications in the detection of different chemical vapours[1-3]. Several sensors, based on conjugated polymers [4, 5], carbon nanostructures [6-8], and related composites [9-12] are attracting attention because of their potential, low cost, high sensitivity, and rapid response to the stimuli. Among various approaches, vapour sensors, based on conductive polymeric composites (CPCs), have emerged as one of the most promising systems. In this type of sensors, polymer acts as the insulating matrix while dispersed conducting particles provide the conducting path through the composite. Carbon nanotubes (CNTs), with almost one-dimensional nanostructure, very high aspect ratio and high conductivity, are ideal as the dispersed particles in conducting particles-insulating matrix composition for gas sensing systems. Hence, CNT/polymer composites have been intensively studied for gas sensors, which have been shown to swell reversibly upon exposure to gases and vapours (analytes). In fact, swelling induces a resistance change in the composite film by increasing the volume of polymer matrix and disrupting some conductive pathways [11]. Once such sensors are exposed to a gaseous analyte, they would interact with at least one of the volatile compounds and thereby, molecular adsorbates can strongly affect the intra and inter carbon nanotube electronic transport properties. The intra-carbon nanotube electronic transport changes are due to charge transfer between the adsorbates molecules and carbon nanotubes [13]. This charge transfer can change the semi-conducting property of CNTs. Based on this mechanism, in some applications semi-

conducting CNTs can be used alone as gas detector. CNTs can only detect molecules having distinct electron donating or accepting abilities [14]. For the detection of molecules that are weakly adsorbed on CNTs surface, the change in resistance is often too small, and thus, their covalent [15, 16] or non-covalent [10] modification is needed. It has been proved that some macromolecules including biopolymers, proteins, nucleic acids and carbohydrates, can smoothly wrap CNTs, and eventually bring them additional functionalities. Instead of chemical modifications, wrapping occurs primarily owing to the combined effect of hydrophobic forces, van der Waals attractions, electrostatic and π-stacking interactions with CNTs[17-20].

The inter CNTs electronic transport changes are due to volumetric changes of the polymer matrix caused by swelling in the presence of interested analyte leading to a distinct change in percolation-type conductivity around a critical composition of the material, which is known as "percolation threshold". This illustrates how polymeric conductive composites combine selectivity and sensitivity from both the carbon nanotube and the polymer matrix. Moreover, Feller et al. proposed the Langmuir – Henry – Clustering (LHC) model which describes the responses in three different analyte concentration regions[9, 21-23]. They found that, solvent molecules meeting the sensor by successive waves would firstly adsorb on macromolecules and CNTs without causing much structural changes than simple perturbations of electrons motion. However, as their amount in the CPC progressively increases, carriers will have to jump by tunnelling due to the increasing gap between CNTs. Afterwards, in the clustering regime induced by high concentration of good solvent molecules, expansion of the conducting network results in a sharp increase in CPC resistance. As a result, conductive particles, and especially CNTs, not only introduce the conductive paths through the composite but also, act as active sites for detection of analytes in CPC transducers. However, the relationships among the nature of the analyte and magnitude response of sensor, composite resistance change, selectivity and polymer swelling are not well known. Several attempts have been made to describe such relationships. For instance, more favourable thermodynamic interactions between the analyte and CPC might lead to higher selectivity [24]. It is clear that affinity is one of the most important parameters that can affect the sensor sensitivity, but some other parameters like the size of penetrant molecule or dielectric constant of analyte can also be influential [25].

In this study, two types of carbon nanotube polymer nanocomposites based on PVA and PEO were fabricated and exposed to different polar vapour analytes including water, methanol, ethanol and isopropyl alcohol (IPA). The responses of the designed nanocomposite sensors were analysed according to the thermodynamic interactions. Furthermore, a novel nanohybrid CPC sensor was designed by wrapping chitosan (Chit) (a polysaccharide biopolymer) around the CNTs. It was demonstrated in the current study that in the case of nanohybrid CPC, the sensitivity to polar vapours is enhanced indicating a more selective adsorption on CNTs. Coupled with this, All-atom Molecular dynamics (MD) was employed to prove the wrapping of chitosan chains around the CNTs and provide detailed information on interactions at the atomistic level.

2 Experimental and Methods

2.1 Materials

Poly (vinyl alcohol) (PVA; Mw = 72000 g mol^{-1}, Sigma Aldrich, Germany) and poly (ethylene oxide) (PEO; Mw = 100000 g mol^{-1}, Sigma Aldrich, Germany) were used as matrices for CPCs. The multiwalled CNTs, synthesized by the thermal chemical vapour deposition (CVD) method, was purchased from CNT Co., LTD, Korea. The average diameters and average lengths of CNTs are 10-40 nm and 1-25 μm, respectively. The purity content was reported to be approximately 93 wt% and the specific surface area was 150-250 m^2 g^{-1}. Medium molecular weight chitosan (molecular weight 280000 g mol^{-1}, degree of deacetylation 83%) was supplied by Fluka. Methanol, ethanol, isopropyl alcohol, chloroform and acetic acid were purchased from Merck (Germany) and used as received.

2.2 Surface decoration of CNTs by chitosan

First, 0.5 wt% chitosan in 1wt% aqueous acetic acid solution was prepared. Chitosan solution was then filtered (vacuum-driven filter with 0.45 μm pore size, Jet Biofil®) to remove any undissolved particles. Afterward, a certain amount of CNTs (3 mg in ml) was added to the solution which then was stirred for 1 hr, and subsequently sonicated in ultrasonic bath for 2 hr. A stable black suspension was obtained which indicates formation of a non-destroyable surface decoration/wrapping of carbon nanotubes with chitosan biopolymer[26, 27].

2.3 Composite Membrane Preparation

Polymer solution (1wt%) was prepared by dissolving of 100 mg PVA or PEO in 100 ml deionized water at 70 °C. Then, a certain amount of decorated CNTs (Chit.CNT) suspension was added to the polymeric solutions. According to the percolation threshold theory, the concentration of CNTs in polymer/CNT composites was fixed at 3 wt%. It was experimentally found that the percolation threshold for PVA/CNT and PEO/CNT in our system was about 2.5 wt%. So the concentration of CNT was selected at 3 wt%, jus near and above the percolation threshold, to get the maximum response and to decrease the noise of response. We used an interdigitated electrode (IE) as a substrate for sensing the conductivity. The gap separation of electrodes (S) was 80 μm. The length (L) and width (W) of each finger are 2 mm and 50 μm, respectively. We assume that $L \gg S$, so that one could neglect end effects at the ends of the electrodes. The spin coater device was used for preparation of a polymeric thin film on IE surface.

2.4 Sensing Apparatus and Measurement

An automatic vapour generation system (AVGS) was used as the sensing apparatus (Figure 1) [28]. This system consists of nitrogen flow, solvent flask (a 100 ml, round-bottomed glass flask), mass flow controllers (MFCs), and a three-way solenoid valve, controlled with a computer. In order to determine the dynamic response of the sensor film to various concentrations of vapours, a portable data acquisition card (DAC Card) (Advantech Ltd., Taiwan) was used. The sensors were exposed to a controlled amount of vapour and, then changes in their DC resistance as a function of time were monitored. The sensors are exposed to nitrogen gas for 5 min to obtain a smooth baseline. Finally, they were exposed to the analyte vapour for 5 min. All the measurements were performed at 25 ± 2 °C.

3 Results and Discussions

3.1 Polymer/CNT nanocomposite sensors

The CNT/polymer sensors including PEO/CNT and PVA/CNT were exposed to different vapour analytes at various vapour concentrations.

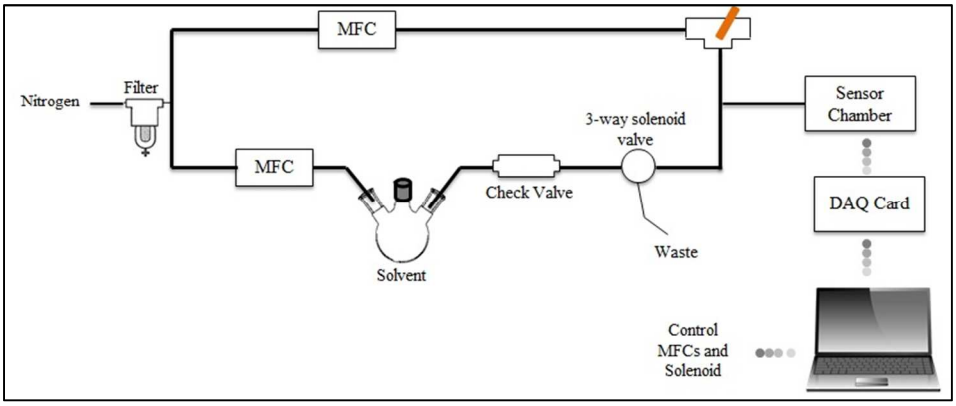

Figure 1. Schematic of an automatic vapour generation system (AVGS)

Figures 2.a and 2.b show the dynamic responses of the designed sensors toward water vapour at different concentrations. The concentrations of water vapour are in a wide range of ppth (part per thousand). As seen, the response time of the sensors is a few seconds and the resistance changes are decreased by lessening the vapour concentration.

The response of a chemiresistor is defined as:

$$\Delta R = \frac{R_{max} - R_b}{R_b} \qquad (1)$$

where R_{max} and R_b indicate the most observed and baseline resistance in each cycle, respectively.

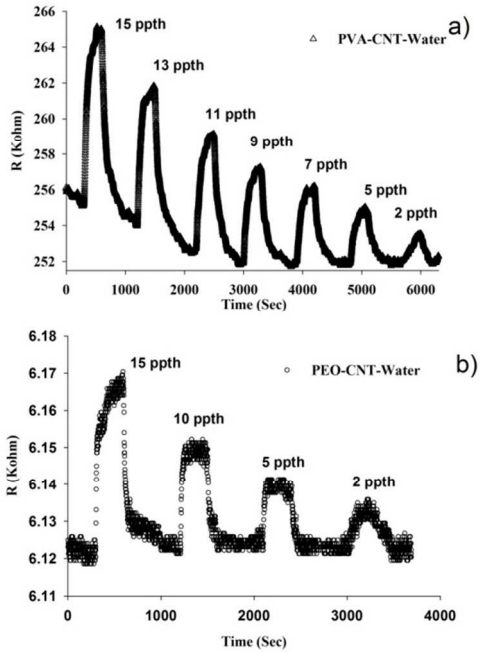

Figure 2. a) Dynamic response of PVA/CNT sensor against different concentrations of water. b) Dynamic response of PEO/CNT sensor against different concentration of water.

Figure 3 demonstrates the selectivity of the designed sensors against various vapours. Figure 3.a displays the PEO/CNT response against 10 ppth of water, ethanol, isopropyl alcohol and chloroform vapours. As shown, the strongest response is observed for water whereas chloroform analyte exhibits the weakest response. Such an observation could be interpreted by the fact that chloroform, being a non-polar solvent, is a solvent for poly (ethylene glycol) (PEG) and low molecular weight PEO. The responses of PVA/CNT sensor exposing to 10 ppth of water, methanol, ethanol and IPA vapours are depicted in Figure 3.b.

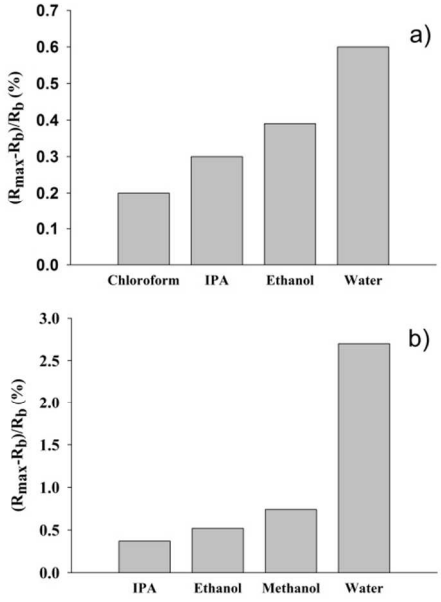

Figure 3. Response of a) PEO/CNT and b) PVA/CNT nanocomposites against 10 ppth of different vapours.

Up to now, there has been reported no comprehensive discussion on how the nature of matrix and analyte correspond to responses; hence, a clear relationship needs to be established.

To elaborate the response behaviours, several thermodynamic interaction parameters are chosen for analytes including Hildebrand solubility parameter and Flory-Huggins (F-H) interaction parameter, as the conventional parameter determining the solubility. Affinity is the most important parameter that can explain the response behaviour of composites against various compounds. Flory-Huggins interaction parameter is the most popular criterion for description of interactions between polymer and solvent.

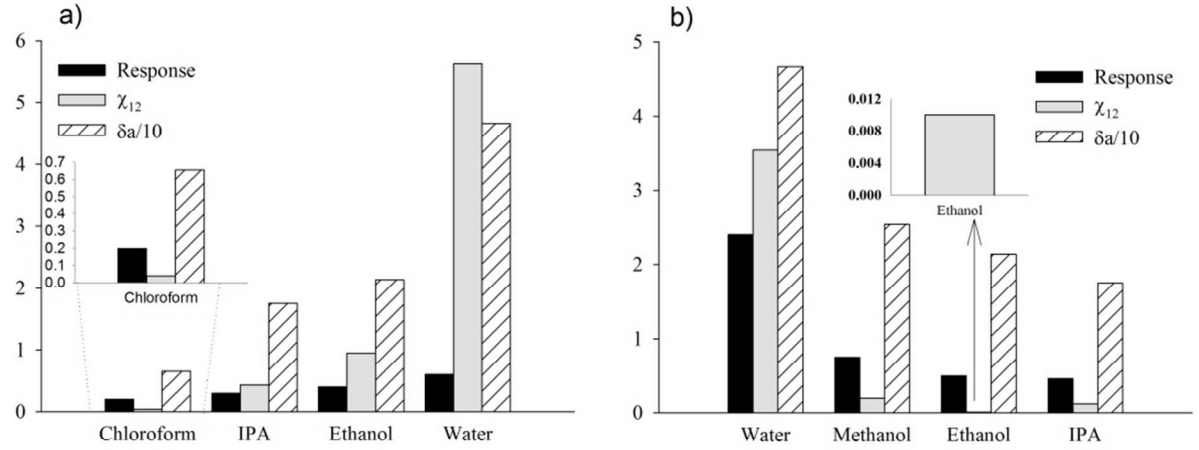

Figure 4. Comparison between response and thermodynamic parameter of polymer matrix and analyte in a) PEO/CNT and b) PVA/CNT nanocomposite sensor. Solubility parameter is in $(J/cm^{-3})^{1/2}$ and response is $\Delta R = \frac{R_{max}-R_b}{R_b}(\%)$

For instance, Choi et al.[29] have interpreted the response magnitude of Polyvinylpyrrolidone (PVP)/CNT sensor against benzene, toluene and O-xylene based on F-H interaction parameter. In another work, by using the F–H interaction parameter, Feller [30] reported the sensitivity of several conductive polymer composites to solvent vapours.

Flory-Huggins interaction parameter is calculated based on Hildebrand solubility parameters:

$$\chi_{12} = \frac{V_M(\delta_p - \delta_s)^2}{RT} \qquad (2)$$

where V_M is the molar volume of solvent, R is the universal gas constant, δ_p and δ_s are Hildebrand solubility parameters for polymer and solvent, respectively, which can be either determined experimentally from P-V-T data or calculated empirically using group contribution methods. The Hildebrand solubility parameters for solvents and polymers used in this study are tabulated in Table 1[31-33], and accordingly, the F-H interaction parameter between polymer and solvents is calculated based on equation 2.

Table 1. The Hildebrand solubility parameter for solvents and polymers and Flory-Huggins interaction parameter between polymer and solvent

	$\delta^{\dagger}$	δ_p	δ_h	δ_d	δ_a	$\chi_{PEO,x}$	$\chi_{PVA,x}$
PEO[32]	19.9	3	9.4	17.3	-	-	-
PVA[33]	26.2	7.8	0.8	25	-	-	-
Methanol[31]	29.6	12.3	22.3	15.1	25.5	-	0.19
Ethanol[31]	26.4	8.8	19.4	15.8	21.3	1.00	0.01
IPA[31]	23.6	6.1	16.4	15.8	17.5	0.42	0.20
Water[31]	47.8	16.0	42.3	15.5	45.2	5.65	3.39
Chloroform[31]	19.0	3.1	5.7	17.8	6.5	0.03	-

†All data for solubility parameters are in $(J\ cm^{-3})^{1/2}$

As can be seen in figure 4, the response trends cannot be described based on the calculated F-H interaction parameters. For PVA/CNT nanocomposite, the following trend could be seen for χ values: $\chi_{12}(\text{ethanol}) < \chi_{12}(\text{IPA}) < \chi_{12}(\text{methanol}) < \chi_{12}$ (water), whereas, the order of response is as follows: $R_{water} \gg R_{methanol} > R_{ethanol} > R_{IPA}$. Although the calculated χ_{12} for water is very high, the best response is surprisingly observed for water. Figure 4 illustrates the same trend which was observed for PEO/CNT composite and χ_{12} is again unable to explain the response order.

In fact, the model of Flory-Huggins and calculated interaction parameters, "Regular Solution Model", could not predict interactions in polar systems. The most important underlying assumptions for this model are (1) no volume changes on mixing, (2) ideal entropy of mixing, and (3) weak forces of the induced dipole type (dispersive interactions). Such formalism implies the interaction parameter χ, purely enthalpic in nature, is always positive and monotonically decreases with increasing temperature, and miscibility only occurs when the solubility parameters of the individual components are of similar magnitude [34]. Therefore, in polar systems and especially those that contain hydrogen bonding, the results of this regular solution model deviate from real value of interaction parameter [35]. There are some complex equations of state for prediction of interaction parameter for systems containing polar or hydrogen bonding interactions[34, 36-39]. Moreover, there also exist many experimental methods for determination of solubility and interaction parameter such as inverse gas chromatography (IGC), turbidimetry, etc[40-42]. It has been reported that the interaction parameters, predicted by these equations of state or obtained by experimental methods, are more reliable as compared to the simple F-H equation. For instance, the interaction parameter of PVA-water has been reported to be 0.494 by means of IGC [43] that is so different from calculated value from equation 2.

It seems that for polar polymers like PVA and PEO, polarity is the most important parameter that can affect the response of sensors, and thus, one can conclude the response of sensors based on polar interactions between polymer and solvents [21]. In fact, δ integrates three types of intermolecular interactions, that are, dispersive, polar and hydrogen bonding; which constitutes the driving force for vapour diffusion through the matrix and finally determines its sensitivity. By plotting the Hanson solubility parameters, it was

observed that with increasing the polar and hydrogen solubility parameter, the sensitivity increased. It is interesting that for these analytes, the increase in sensitivity corresponds to increase in δ_a, which is the vector sum of δ_h and δ_p:

$$\delta_a^2 = \delta_h^2 + \delta_p^2 \qquad (3)$$

For water and PEO/CNT nanocomposite, a sharp increase in δ, was detected; however, sensitivity exhibited no significant increase. The reason for this behaviour may lie in the nature of PEO matrix consisting of ether groups on the backbone and OH moieties at the tails. By increasing the molecular weight, the density of OH moieties decreased, leading to weaker hydrogen interactions. Therefore, although water has a high δ_a, the sensitivity does not correspond to increase in δ_a because of insufficient available OH moieties. It implies that as the molecular weight of PEO decreases, the sensitivity is increased.

3.2 CNTs decoration

As discussed above, the polar Hansen parameters contribute to a better response for polar solvents allowing one to select a polar macromolecule to modify the sensors. Owing to its high polar nature and wrapping capability, chitosan was chosen to modify the CNTs and design nanohybrid polymeric composites. Chitosan has distinct hydrophilicity due to the existence of high proportion of amino and hydroxyl functional groups, and thus, exhibits a high capability for improving the sensitivity of nanocomposites to polar analytes. The dispersion and solubility of CNTs can be remarkably improved through substantial wrapping of chitosan owing to the emulsifying capacity of chitosan [27]. Chitosan macromolecules in acidic solutions possess $NH3^+$ groups that can wrap CNTs providing active polar sites in its vicinity. Such polar sites allow for more interactions between the polar analytes and CNTs.

Molecular dynamics (MD) simulation was employed to study different interactions between CNTs, chitosan chains and the polymer matrix. Molecular dynamics simulations were carried out on Materials Studio (Discover and Amorphous Cell modulus) developed by Accelrys Software Inc. Three amorphous cell models for random initial distributions of CNT-Chit, PVA-Chit.CNT and PEO-Chit.CNT nanocomposite membrane were constructed and shown in Figs. 5.a, b and c. The details about the molecular dynamics simulation can be found in Appendix. Figure 5.d illustrates the CNT-Chit structure after simulation. As can be seen, chitosan macromolecules wrapped the CNTs and made a thin layer on its surface. Chitosan macromolecules have a tendency for spontaneous wrapping around tubular surfaces of CNTs. Polymers with stiff and semi flexible backbones tend to adhere to the CNTs and the stiffness in these backbones decreases the intra-chain coiling in most cases[44]. Moreover, chitosan macromolecules take helical conformation because of van der Waals attractions and favoured free-energy [45]. The final state of chitosan chains in PEO-Chit.CNT and PVA-Chit.CNT nanocomposites is illustrated in Figures 5.e and f. In these figures, PEO and PVA chains have been omitted for clarity. It is obvious that, chitosan macromolecules retain their tendency to CNTs even in the presence of PEO and PVA macromolecules. This interaction between CNTs and chitosan biopolymer appears to be weak in the presence of PVA. It is possibly because of the hydrogen bonding potential between chitosan and PVA, and also, long relaxation time of PVA in comparison with the time scale of simulation. It is possible that in a longer simulation time, chitosan molecules become more close to CNTs as well. Therefore, this simulation indicated the construction of active sites on CNTs surfaces by chitosan decoration while retaining the essential conductivity properties.

3.3 Polymer / Chit.CNT nanocomposite sensors

Figures.6.a and 6.b illustrate the response of PEO/Chit.CNT and PVA/Chit.CNT against various concentrations of water. As shown, the response is very fast and returns immediately to the baseline after switching the flow from solvent to pure nitrogen. Figures 6.c and d are a comparison between response of sensor nanocomposites with and without chitosan decoration versus different concentrations of water vapours. As seen, non-covalent modification of CNTs by chitosan improved the response and sensitivity of these chemiresistors against polar molecules of water vapour. These modified transducers were introduced to polar and non-polar analytes in various concentrations and their response were compared with the un-modified sensors. Figure 7 illustrates the response of the chemiresistors against 10 ppth concentration of different vapours. As can be seen, by introducing the chitosan molecules to conductive nanocomposite membranes, the response of sensors against polar vapours is enhanced. Based on LHC model that was proposed by Feller et al.[9, 21] in the case of CPC transducers, CNTs can act as active sites for adsorption of analytes. According to LHC model, in intermediate concentration of analytes, adsorption of vapour molecules on CNTs surfaces and local disconnection of conductive pathways as well as swelling can be responsible for the response magnitude. Therefore, by wrapping of CNTs with chitosan, the polar pendant groups of chitosan enhanced the driving force of diffusion of polar molecules into the nanohybrid composite and adsorption on the surface of CNTs. By increasing the amount of adsorbent analytes on the surface of CNTs, local plasticization of polymer chains disrupted the electron tunnelling between CNTs. Consequently, the resistance changes due to diffusion of analyte were increased. It could be evidently manifested from Figure 7 that the response magnitude of PVA/Chit.CNT increased from 2.4 to 5 against water vapour, and from 0.75 to 1.3 against methanol vapour.

However, a decrease in the response of PEO/Chit.CNT versus chloroform is observed. Although chloroform is non-polar, it is a good solvent for PEG and low molecular weight PEO. So, the PEO/CNT sensors have a good response against chloroform. Nevertheless, by wrapping of polar macromolecules around CNTs, the driving forces for diffusion and tendency of chloroform molecules into the nanocomposite membrane have been decreased affecting the response of the fabricated chemiresistor.

4 Conclusion

We used poly (ethylene oxide) and poly (vinyl alcohol) as matrices in carbon nanotube nanocomposite vapour sensors. The chemiresistors were introduced to various organic vapours such as methanol, ethanol, isopropyl alcohol, chloroform and water. The response of sensors was investigated based on thermodynamic parameters. The simple model of χ, which was proposed by Flory and Huggins, cannot explicate the interactions in polar systems. For instance, for PVA/CNT nanocomposite, the following trend could be seen for χ values: $\chi_{12}(\text{ethanol}) < \chi_{12}(\text{IPA}) < \chi_{12}(\text{methanol}) < \chi_{12}$ (water), whereas, the order of response is as follows: $R_{water} \gg R_{methanol} > R_{ethanol} > R_{IPA}$. Consequently, the response trend of transducers was interpreted based on δ_a, which is the vector sum of δ_p and δ_h (polar and hydrogen bonding contribution of Hansen solubility parameter). It has been demonstrated that by increasing the polarity of analytes, the interaction with PVA and PEO improved, and thus, the transducer had a better response. Moreover, by designing a new hybrid nanocomposite, the sensor response against polar vapours was improved. New active sites were introduced by wrapping of CNTs with chitosan. Decoration of CNTs by chitosan increased the sensitivity of these sensors against polar solvents. This decoration was further proved by molecular dynamics simulations.

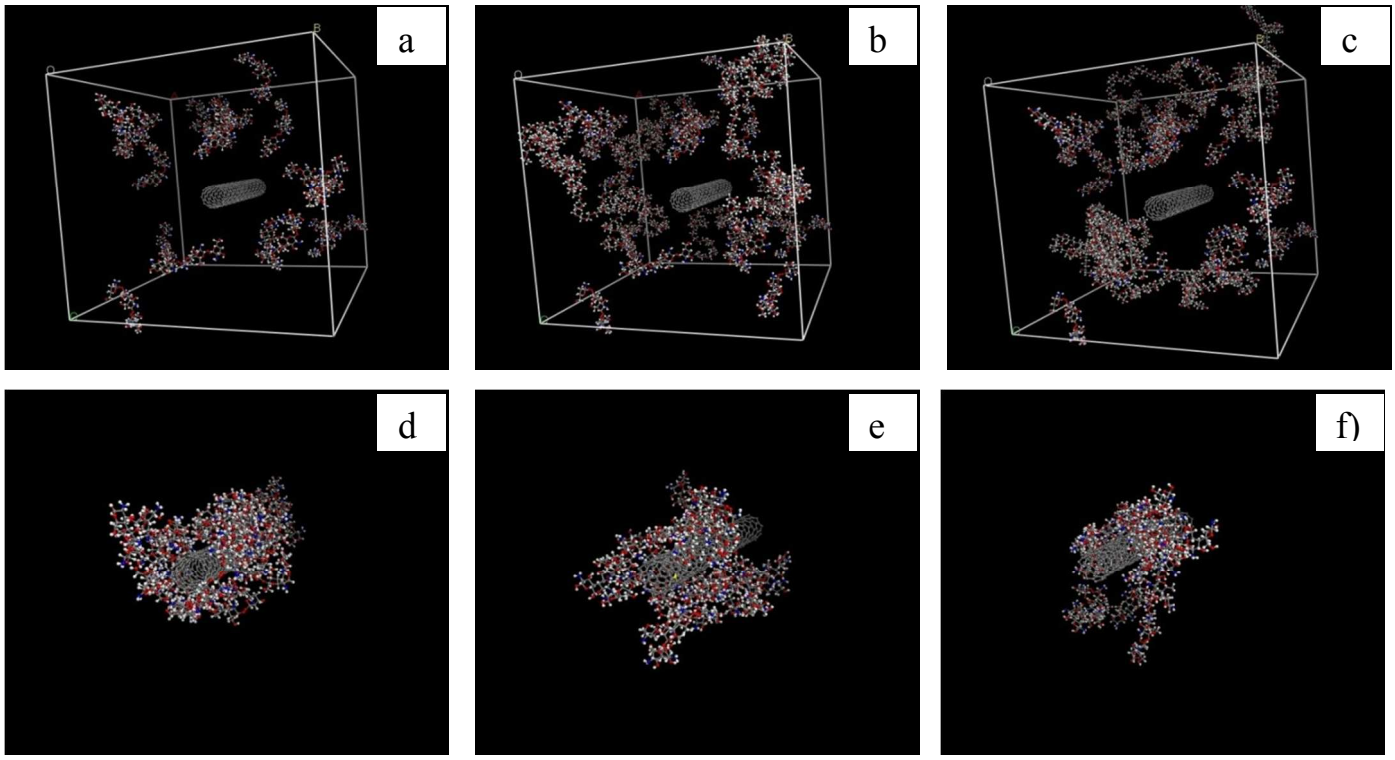

Figure 5. a, b and c: Three amorphous cell models for random initial distributions of CNT-Chit, PEO-Chit.CNT, and PVA-Chit.CNT nanocomposite membrane respectively, and final structure of d) CNT-Chit, e) PEO-Chit.CNT, and f) PVA-Chit.CNT. (In figures e and f PVA and PEO macromolecules are omitted for better clarity.) All atoms are display in form of "Ball and Stick". For all samples the colour code is: carbon: grey; oxygen: red; hydrogen: white; nitrogen: blue. (For interpretation of the references to colour in this figure legend, the reader referred to the web version of this article.)

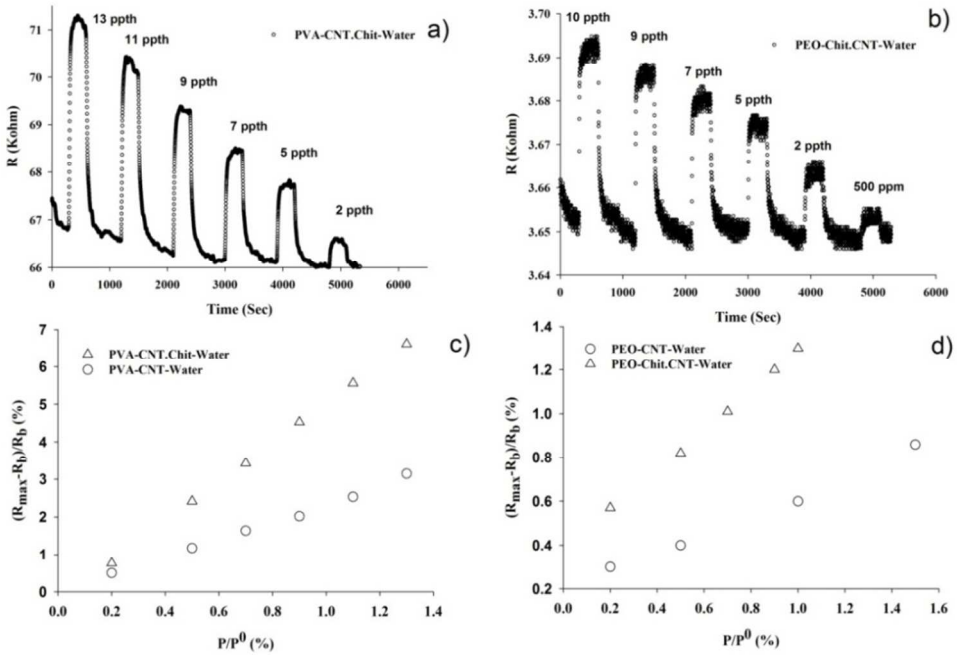

Figure 6. Response of a) PVA/Chit.CNT and b) PEO/Chit.CNT against various concentrations of water. Response of sensor nanocomposites with and without chitosan decoration versus different concentrations of water vapours in c) PVA/Chit.CNT and d) PPEO/Chit.CNT

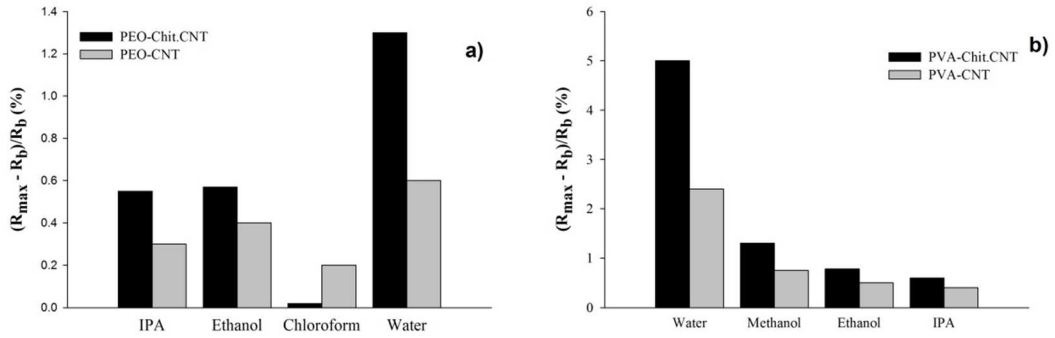

Figure 7. Comparison between sensor responses against 10 ppth concentration of different vapours in a) PEO/Chit.CNT and b) PVA/Chit.CNT with and without non-covalent modification

Acknowledgements

The authors would like to thank Dr. E.Danesh for his inspirations and Dr. G.Bahlakeh for his helpful assistance in Molecular Dynamics Simulations. Gratitude is also expressed to M.Janmaleki from "*Nanomedicine and Tissue Engineering Research Center, Shahid Beheshti University (M.C.)*" for his helpful technical assistance. We also gratefully acknowledge valuable scientific discussions with Tahereh Aghaali and E.Dashtimoghadam for critical review of the manuscript.

Appendix. Molecular dynamics simulation Details

In order to examine the wrapping properties of chitosan biopolymers around CNT, five different systems were studied by using molecular dynamics (MD) simulations. These simulation systems include Chit-CNT-PVA, PVA-Chit, Chit-CNT- PEO, PEO-Chit and Chit-CNT. For this purpose, five three-dimensional (3D) cubic amorphous simulation cells were constructed by means of Amorphous Cell module of Materials Studio software [46]. In construction of these 3D amorphous cells, four chains of PVA and PEO polymers each with degree of polymerization of 100, twenty chains of chitosan with chain length of 5, and a single-walled CNT (10,0) of diameter 7.83 Å and length 46.86 Å were used.

COMPASS (Condensed-Phase Optimized Molecular Potentials for Atomistic Simulation Studies) force field, which is the first ab initio force field, was employed for simulation of all molecules. Velocity Verlet integration method was applied to solve Newton equation of motion with time step of 1 fs (10-15 s). Non-boned interactions among the molecules were taken into account by Ewald summation method.

In order to better equilibrate the 3D cells and remove the dependency of simulation on the initial structure, starting cells were generated at low density of 0.1 g cm-3, as shown in Figure 5. All constructed initial simulation cells were first optimized for 5000 steps with the use of Smart minimizer algorithm as implemented in Materials Studio software. The energy-optimized structures were then simulated at highest temperature of 700 K for at least 50 ps under NPT ensemble. Afterwards, MD simulations were continued with successive reduction of temperature until 300 K in intervals of 50 K. At each temperature, simulations were performed for time period of 50 ps. This simulation procedure was adopted to accelerate the achievement of equilibrated cells. The final cell obtained from NPT MD simulation at 300 K was further simulated in NVT ensemble for 250 ps. During NPT and NVT simulations, pressure and temperature were controlled with Berendsen barostat (at 1 atmosphere) and Andersen thermostat, respectively. All MD simulations were carried out by using Materials Studio software[46].

Notes and references

1. M. Castro, B. Kumar, J. F. Feller, Z. Haddi, A. Amari and B. Bouchikhi, *Sensors and Actuators B: Chemical*, 2011, **159**, 213-219.
2. M. W. C. C. Greenshields, M. A. Mamo, N. J. Coville, A. P. Spina, D. F. Rosso, E. C. Latocheski, J. G. Destro, I. C. Pimentel and I. A. Hümmelgen, *Journal of Agricultural and Food Chemistry*, 2012, **60**, 10420-10425.
3. G. Konvalina and H. Haick, *Accounts of Chemical Research*, 2013.
4. A. L. Kukla, A. S. Pavluchenko, Y. M. Shirshov, N. V. Konoshchuk and O. Y. Posudievsky, *Sensors and Actuators B: Chemical*, 2009, **135**, 541-551.
5. Q. Ameer and S. B. Adeloju, *Sensors and Actuators B: Chemical*, 2005, **106**, 541-552.
6. N. Peng, Q. Zhang, Y. C. Lee, O. K. Tan and N. Marzari, *Sensors and Actuators B: Chemical*, 2008, **132**, 191-195.
7. M. Lucci, A. Reale, A. Di Carlo, S. Orlanducci, E. Tamburri, M. L. Terranova, I. Davoli, C. Di Natale, A. D'Amico and R. Paolesse, *Sensors and Actuators B: Chemical*, 2006, **118**, 226-231.
8. O. K. Varghese, P. D. Kichambre, D. Gong, K. G. Ong, E. C. Dickey and C. A. Grimes, *Sensors and Actuators B: Chemical*, 2001, **81**, 32-41.
9. B. Kumar, J.-F. Feller, M. Castro and J. Lu, *Talanta*, 2010, **81**, 908-915.
10. B. Kumar, M. Castro and J.-F. Feller, *Carbon*, 2012, **50**, 3627-3634.
11. M. C. Lonergan, E. J. Severin, B. J. Doleman, S. A. Beaber, R. H. Grubbs and N. S. Lewis, *Chemistry of Materials*, 1996, **8**, 2298-2312.
12. P. Molla-Abbasi, S. R. Ghaffarian and E. Danesh, *Smart Materials and Structures*, 2011, **20**, 105012.
13. M. W. C. C. Greenshields, M. S. Meruvia, I. A. Hümmelgen, N. J. Coville, S. D. Mhlanga, H. J. Ceragioli, J. C. Rojas Quispe and V. Baranauskas, *Journal of Nanoscience and Nanotechnology*, 2011, **11**, 2384-2388.

14. S. Peng and K. Cho, *Nanotechnology*, 2000, **11**, 57.
15. Y. Zilberman, U. Tisch, G. Shuster, W. Pisula, X. Feng, K. Müllen and H. Haick, *Advanced Materials*, 2010, **22**, 4317-4320.
16. Y. Wang, H. Xiong, Y. Gao and H. Li, *J Mater Sci*, 2008, **43**, 5609-5617.
17. S. Jung, M. Cha, J. Park, N. Jeong, G. Kim, C. Park, J. Ihm and J. Lee, *Journal of the American Chemical Society*, 2010, **132**, 10964-10966.
18. I. Gurevitch and S. Srebnik, *Chemical Physics Letters*, 2007, **444**, 96-100.
19. M. M. Hasani-Sadrabadi, E. Dashtimoghadam, F. S. Majedi, H. Moaddel, A. Bertsch and P. Renaud, *Nanoscale*, 2013, **5**, 11710-11717.
20. M. M. Hasani-Sadrabadi, E. Dashtimoghadam, F. S. Majedi, S. Wu, A. Bertsch, H. Moaddel and P. Renaud, *RSC Adv.*, 2013, **3**, 7337-7346.
21. A. Bouvree, J.-F. Feller, M. Castro, Y. Grohens and M. Rinaudo, *Sensors and Actuators B: Chemical*, 2009, **138**, 138-147.
22. J. F. Feller and Y. Grohens, *Synthetic Metals*, 2005, **154**, 193-196.
23. M. Castro, J. Lu, S. Bruzaud, B. Kumar and J.-F. Feller, *Carbon*, 2009, **47**, 1930-1942.
24. P. Jurs, G. Bakken and H. McClelland, *Chemical Reviews*, 2000, **100**, 2649-2678.
25. J. Lu, B. Kumar, M. Castro and J.-F. Feller, *Sensors and Actuators B: Chemical*, 2009, **140**, 451-460.
26. M. Zhang, A. Smith and W. Gorski, *Analytical Chemistry*, 2004, **76**, 5045-5050.
27. F. Peng, F. Pan, H. Sun, L. Lu and Z. Jiang, *Journal of Membrane Science*, 2007, **300**, 13-19.
28. E. Danesh, S. R. Ghaffarian and P. Molla-Abbasi, *Sensors and Actuators B: Chemical*, 2011, **155**, 562-567.
29. J. Choi, D. W. Park and S. E. Shim, *Synthetic Metals*, 2012, **162**, 1513-1518.
30. J. F. Feller and Y. Grohens, *Sensors and Actuators B: Chemical*, 2004, **97**, 231-242.
31. C. M. Hansen, *Hansen solubility parameters: a user's handbook*, CRC press, 2007.
32. A. Chan, K. Coppens, M. Hall, V. He, P. Jog, P. Larsen, B. Koblinksi, M. Read, D. Rothe and S. Somasi, 2006 American Association of Pharmaceutical Scientists Annual Meeting and Exposition, San Antonio, TX, 2006.
33. A. F. Barton, *CRC handbook of polymer-liquid interaction parameters and solubility parameters*, CRC press, 1990.
34. A.-V. G. Ruzette and A. M. Mayes, *Macromolecules*, 2001, **34**, 1894-1907.
35. C. Panayiotou and I. Sanchez, *The Journal of Physical Chemistry*, 1991, **95**, 10090-10097.
36. X. Kong, M. D. L. V. Silveira, L. Zhao and P. Choi, *Macromolecules*, 2002, **35**, 8586-8590.
37. S. T. Milner, M.-D. Lacasse and W. W. Graessley, *Macromolecules*, 2009, **42**, 876-886.
38. C. Panayiotou and I. C. Sanchez, *The Journal of Physical Chemistry*, 1991, **95**, 10090-10097.
39. Y. Park, B. Veytsman, M. Coleman and P. Painter, *Macromolecules*, 2005, **38**, 3703-3707.
40. K. W. Suh and J. M. Corbett, *Journal of Applied Polymer Science*, 1968, **12**, 2359-2370.
41. E. Díez, G. Ovejero, M. D. Romero and I. Díaz, *Fluid Phase Equilibria*, 2011, **308**, 107-113.
42. M. Kunaver, J. Zadnik, O. Planinsek and S. Srcic, *Acta chimica slovenica*, 2004, **51**, 373-394.
43. J. E. Mark, *Physical properties of polymers handbook*, Springer, 2007.
44. S. S. Tallury and M. A. Pasquinelli, *The Journal of Physical Chemistry B*, 2010, **114**, 9349-9355.
45. Y. Liu, C. Chipot, X. Shao and W. Cai, *The Journal of Physical Chemistry C*, 2011, **115**, 1851-1856.
46. D. Studio, *San Diego, CA*, 2009, **92121**.

Table of contents:

Color graphic:

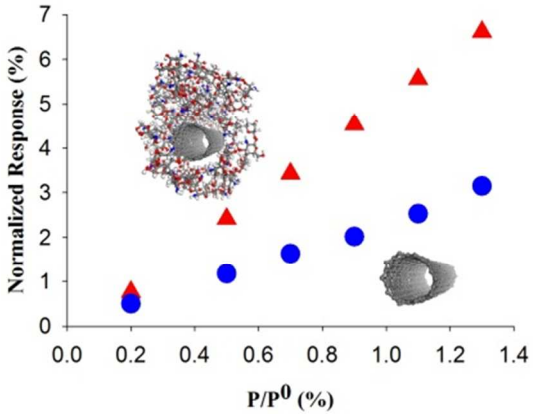

Text: A new hybrid nanocomposite was designing by introducing the decorated CNT into polymer for improving the sensitivity against polar vapors.